SCIENCE CHINA
Information Sciences

• RESEARCH PAPER •

January 2026, Vol. 69, Iss. 1, 112208:1–112208:17
https://doi.org/10.1007/s11432-024-4529-9

Hierarchical control of nonholonomic wheeled mobile robot based on atan3

Zhaojing WU* & Likang FENG

School of Mathematics and Informational Science, Yantai University, Yantai 264005, China

Received 1 September 2024/Revised 8 April 2025/Accepted 14 May 2025/Published online 4 January 2026

Abstract A unified controller for trajectory tracking and set-point regulation/stabilization of nonholonomic wheeled mobile robots is designed by using the hierarchical idea popular in unmanned aerial vehicles. As a preliminary, a smooth function for solving the argument of a rotating vector is obtained by switching between discontinuous functions, which motivates the definition of a novel function atan3. The hierarchical control is introduced to wheeled mobile robots, which includes an attitude planner based on atan3, nominal full-actuated position control, and planner-based attitude control, such that the exponential stability of the closed-loop system is achieved. It is easy to extend the control of nonholonomic wheeled mobile robots (WMRs) with unknown parameters and disturbances. The simulation results demonstrate the effectiveness of the control scheme and the necessity of introducing the function atan3.

Keywords switching, nonholonomic systems, hierarchical control, wheeled mobile robot, atan3

Citation Wu Z J, Feng L K. Hierarchical control of nonholonomic wheeled mobile robot based on atan3. Sci China Inf Sci, 2026, 69(1): 112208, https://doi.org/10.1007/s11432-024-4529-9

1 Introduction

Nonholonomic wheeled mobile robots (WMRs) are under-actuated systems with non-integrable constraints on the speeds, which cannot be stabilized by continuous time-invariant state feedback due to Brockett's condition [1]. The existing literature on control for nonholonomic systems is mainly about set-point regulation/stabilization, tracking, and unification of them [2, 3]. For the stabilization of WMRs or more general nonholonomic systems, a variety of control methods have been proposed. A piecewise analytic strategy was provided for transferring an arbitrary initial state of a Chaplygin system to the origin in [4], and a piecewise smooth controller was constructed for WMRs to achieve exponential stabilization in [5]. A local exponential stability result was obtained using a continuous time-varying control law [6]. Global asymptotic feedback controllers were proposed for a class of nonholonomic systems by introducing time-varying terms in [7, 8]. To overcome the slow asymptotic response, Refs. [9, 10] constructed time-varying homogeneous feedback controllers to achieve globally asymptotic and locally exponential stability for nonholonomic systems. For other developments about the stabilization of nonholonomic systems, please refer to [11–15].

For the trajectory tracking problem of WMRs, several controllers were also proposed. Time-varying state feedback tracking controllers were proposed by using the backstepping technique for nonholonomic systems in [16, 17]. For nonholonomic WMRs with uncertainties, an adaptive controller was presented in [18], a robust adaptive controller was proposed with the aid of the learning ability of neural networks in [19], and an adaptive output feedback tracking controller was presented in [20]. For nonholonomic WMRs using only measurements for position and velocity, a trajectory tracking controller was designed based on a full-order observer and a filter in [21].

To the unified methods for both set-point regulation/stabilization and trajectory tracking, much attention has been paid. A discontinuous unified control scheme was presented for the kinematic model of WMRs in [22], and a time-varying controller with internal dynamics was designed for the kinematic model in [23]. In [24], a unified tracking and regulation controller was presented by introducing some time-varying auxiliary signals to avoid switching action. Do et al. [25] solved both adaptive tracking and stabilization simultaneously by introducing an error rotation transformation for WMRs. A saturated time-varying controller was developed by applying a novel error state modification with bounded auxiliary variables in [26].

* Corresponding author (email: wuzhaojing00@188.com, wzj00@ytu.edu.cn)

In the above literature on the trajectory tracking of WMRs, the desired position and attitude come from the reference model. In reality, the tracking target often contains only position information, which requires the controller to have the maneuverability to produce the desired attitude. This inspires us to introduce the hierarchical control for WMRs, which is widely used in controls of unmanned aerial vehicles (UAVs); please see [27–30].

For the dynamic model of nonholonomic WMRs, a hierarchical control is designed for trajectory tracking and stabilization in this paper. The main contribution consists of the following aspects.

(i) A discontinuous function is smoothed via switching to calculate the argument angle of a rotating vector, which leads to the definition of atan3, regarded as a generalization of atan2.

(ii) An attitude planner is constructed with the aid of atan3 such that the trajectory tracking and stabilization are transformed to full-actuated position controls.

(iii) A hierarchical design results in a smooth and time-invariant control, the exponential stability of the closed-loop error system, and the convenience of an adaptive law for all unknown system parameters.

This result does not contradict Brockett's condition because only the desirable position is tracked, and the attitude is produced by a planner.

2 Problem formulation and mathematical preliminary

2.1 Description of nonholonomic robots

In this paper, the trajectory control problem of nonholonomic WMRs is considered, as shown in Figure 1. P_o is the middle point between the left and right wheels, and P_c is the center of the mass of the robot. Let l_w be the radius of each wheel, l_b be the distance from P_o to the left (right) wheel center, and l_d be the distance between P_o and P_c. m_c and m_w are the masses of the body and wheel, respectively. I_c, I_w and I_m are the moments of inertia of the body about the vertical axis through P_o, the wheel with a motor about the wheel axis, and the wheel with a motor about its diameter, respectively. The nonnegative constant d_p is the coefficient of the damping to one wheel.

Let $r = (x, y)^\top$ denote the coordinate of P_o in XOY plane, and let ψ denote the yaw angle of the body around the point P_o. Let v and w denote the linear and angular velocities of the robot, respectively. τ_1 and τ_2 denote the torques provided by direct current (DC) motors on the left and right wheels, respectively. In this paper, for the sake of simplicity, we assume that the robot does not slip and there is no sliding between the tires and the road.

A dynamic equation of WMRs was introduced by Sarkar et al. [31], and was rewritten by Huang et al. [20, Eqs. (5)–(8)], in the form of

$$\begin{aligned} &\dot{\eta} = L(\eta)\varpi, \\ &M\dot{\varpi} = -C(\omega)\varpi - D\varpi + B\tau, \end{aligned} \tag{1}$$

where $\eta = [x, y, \psi]^\top$, $\varpi = [v, \omega]^\top$, $\tau = [\tau_1, \tau_2]^\top$, and matrices $L(\eta), M, C(\omega), D$ and B are given as

$$L(\eta) = \begin{bmatrix} \cos\psi & 0 \\ \sin\psi & 0 \\ 0 & 1 \end{bmatrix}, \quad M = \begin{bmatrix} m_1 & 0 \\ 0 & m_2 \end{bmatrix}, \quad B = \tfrac{l_w}{2l_b}\begin{bmatrix} 1 & 1 \\ l_b & -l_b \end{bmatrix},$$

$$C(\omega) = \begin{bmatrix} 0 & k_0\omega \\ -k_0\omega & 0 \end{bmatrix}, \quad D = \begin{bmatrix} \dfrac{d_p}{l_b} & 0 \\ 0 & l_b d_p \end{bmatrix}$$

with

$$\begin{aligned} m_1 &= \frac{1}{2l_b} l_w^2 (m_c + 2m_w) + I_w, \\ m_2 &= \frac{1}{2l_b} l_w^2 (m_c l_d^2 + 2m_w l_b^2 + I_c) + I_w + 2I_m, \\ k_0 &= \frac{1}{2l_b} l_w^2 m_c l_d. \end{aligned}$$

For the convenience of hierarchical control design, the dynamic equation is rewritten as

$$\text{Position}: \begin{cases} \dot{r} = v\Lambda(\psi), \\ \dot{v} = p_1 F - \dfrac{k_0}{m_1}\omega^2 - k_1 v, \end{cases} \tag{2a}$$

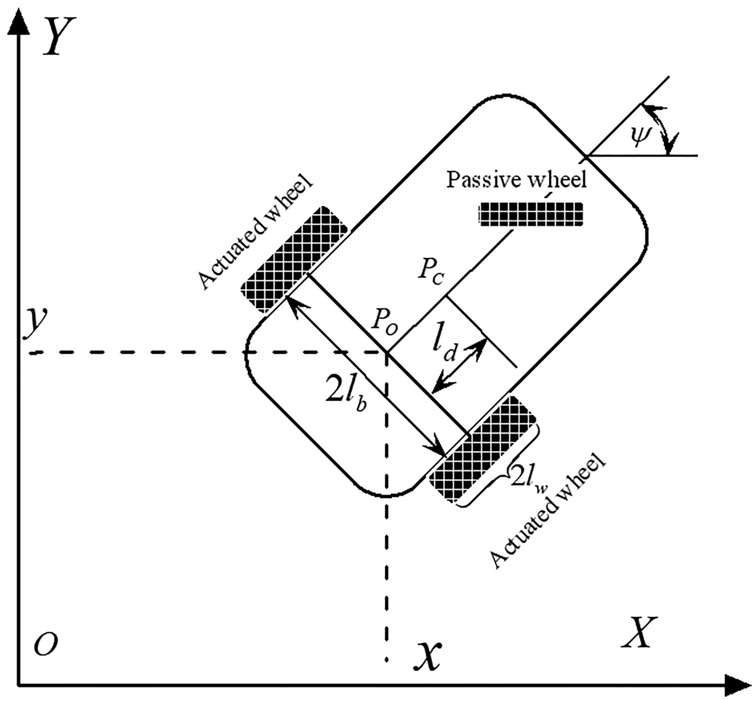

Figure 1 Nonholonomic WMRs.

$$\text{Attitude}:\begin{cases}\dot{\psi}=\omega,\\ \dot{\omega}=p_2\Gamma+\dfrac{k_0}{m_2}v\omega-k_2\omega,\end{cases}\tag{2b}$$

where

$$r=[x,y]^\top,\quad \Lambda(\psi)=[\cos\psi,\sin\psi]^\top,$$
$$p_1=\frac{l_w}{l_bm_1},\quad p_2=\frac{l_w}{m_2},\quad k_1=\frac{d_p}{l_bm_1},\quad k_2=\frac{d_pl_b}{m_2},$$
$$F=\frac{1}{2}(\tau_1+\tau_2),\quad \Gamma=\frac{1}{2}(\tau_1-\tau_2).$$

Control objective. Given a reference position r_* whose first two order derivatives are continuous and bounded functions, the control τ in (1) is designed so that $r(t)$ can track the desired position r_*.

Remark 1. The control objective is presented in the form of trajectory tracking, but when r_* is a constant vector, this problem reduces to the set-point regulation/stabilization.

2.2 Smoothed switch and atan3

For a point A with coordinate (x,y) in XOY plane, the principal argument of vector $\overrightarrow{OA}$ can be calculated via arctangent function $\operatorname{atan}(y/x)$ with range $(-\pi/2,\pi/2)$. To overcome zero division on the Y axis, function $\operatorname{atan2}(y,x)$[1] is introduced as

$$\operatorname{atan}2(y,x)=\begin{cases}\dfrac{\pi}{2}(1-\operatorname{sign}(x))\operatorname{sign}(y)+\operatorname{atan}\left(\dfrac{y}{x}\right), & x\neq 0,\\ \dfrac{\pi}{2}\operatorname{sign}(y), & x=0\end{cases}$$

with range $[-\pi,\pi)$.

1) Function atan2 can be traced back to the FORTRAN-language [32], which is now widely used in many fields. For example, it can be found in the math.h file of the math standard library of the C-language, the system.math file of the Java math library, and the math module of Python.

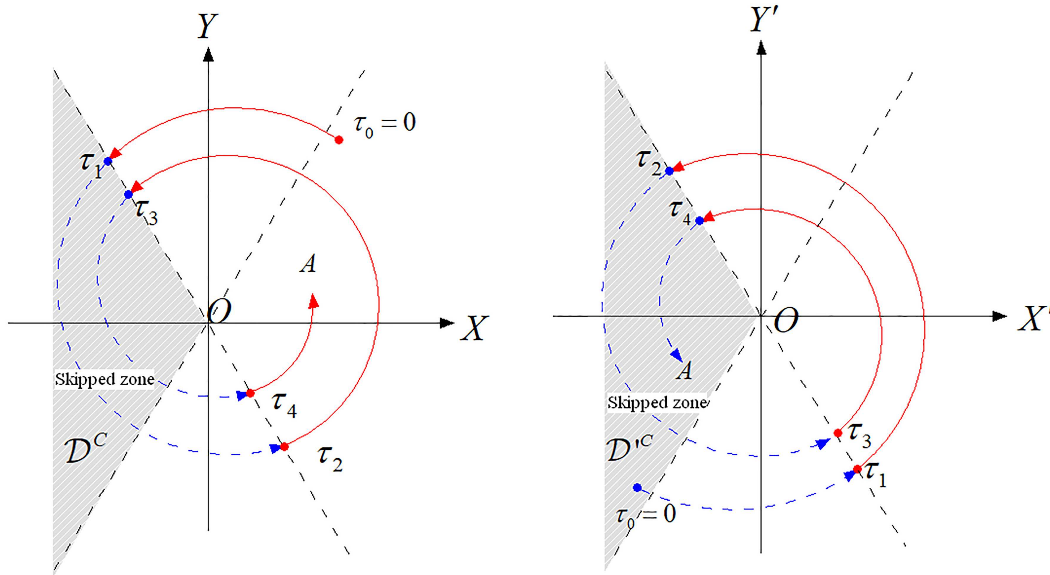

Figure 2 (Color online) In original coordinate axis (left) and flipped coordinate axis (right), the shaded areas are the skipped zones, the solid lines represent the paths passed through, and the dashed lines represent the skipped paths.

Turn to the case that A moves smoothly with time-varying coordinate $(x(t), y(t))$, and consider the calculation of argument $\psi(t)$ of vector $\overrightarrow{OA}$, which is different from the principle value

$$\bar{\psi}(t) = \text{atan2}(y(t), x(t))$$

in general. To this end, the original coordinate XOY is rotated 180° around point O to the frame $X'OY'$ with expression $(x'(t), y'(t)) = (-x(t), -y(t))$, and is named as the flipped coordinate, as shown in Figure 2. In order to avoid applying atan2 to the points on negative X (or X')-axis, interval $[-2\pi/3, 2\pi/3]$ (or $[-3\pi/4, 3\pi/4]$ or $[-4\pi/5, 4\pi/5]$), is chosen to define active zones:

$$\mathcal{D} = \left\{(x, y) : \text{atan2}(y, x) \in \left(-\frac{2}{3}\pi, \frac{2}{3}\pi\right)\right\},$$
$$\mathcal{D}' = \left\{(x', y') : \text{atan2}(y', x') \in \left(-\frac{2}{3}\pi, \frac{2}{3}\pi\right)\right\},$$

whose complementary sets $\mathcal{D}^C$ and $\mathcal{D}'^C$ are called skipped zones. The first exit time from $\mathcal{D}$ is

$$\tau_1 = \inf\{t \geqslant \tau_0 : (x(t), y(t)) \in \mathcal{D}^C\}, \quad \tau_0 = 0$$

with $\inf \emptyset = \infty$ (the same is omitted below). After the finite moment τ_1, coordinate system $X'OY'$ is active until $(x'(t), y'(t))$ leaves $[-2\pi/3, 2\pi/3]$, which leads to the first exit time from $\mathcal{D}'$,

$$\tau_2 = \inf\{t \geqslant \tau_1 : (x'(t), y'(t)) \in \mathcal{D}'^C\},$$

and recursively

$$\begin{aligned} \tau_{2m-1} &= \inf\{t \geqslant \tau_{2m-2} : (x(t), y(t)) \in \mathcal{D}^C\}, \\ \tau_{2m} &= \inf\{t \geqslant \tau_{2m-1} : (x'(t), y'(t)) \in \mathcal{D}'^C\} \end{aligned} \tag{3}$$

(see Figure 2). Thus, an indicator function about the active frame is presented as

$$\sigma(t) = \begin{cases} 1, & t \in [\tau_{2m-2}, \tau_{2m-1}), \\ -1, & t \in [\tau_{2m-1}, \tau_{2m}), \ m = 1, 2, \ldots, \end{cases} \tag{4}$$

which means that the active coordinate is XOY if $\sigma(t) = 1$ and $X'OY'$ if $\sigma(t) = -1$. Regarding (4) as a switching signal, the corresponding principal argument is presented as

$$\phi(t) = \text{atan2}(\sigma(t)y(t), \sigma(t)x(t)), \tag{5}$$

which is a piecewise continuous function with step $\pm\pi$ at discontinuities τ_i.

The algebraic sum of switches of the coordinate frames up to time t is

$$s(t) = \sum_{0 \leqslant \tau_i \leqslant t} \mathrm{sign}(\phi(\tau_i)), \tag{6}$$

which means that the angle lost due to switching equals $s(t)\pi$. Finally, the argument is obtained by adding the lost angle to the principal value, i.e.,

$$\psi(t) = \phi(t) + s(t)\pi. \tag{7}$$

Denoting the operation of argument by a symbol atan3 gives

$$\mathrm{atan3}(x(t), y(t), \sigma(t)) = \phi(t) + \pi \sum_{0 \leqslant \tau_i \leqslant t} \mathrm{sign}(\phi(\tau_i)), \tag{8}$$

which is a generalization of atan and atan2 to the smooth case. The notion atan3 is used to emphasize the dependence on the continuous state $(x, y) \in \mathbb{R}^2$ and a jump model $\sigma(t) \in \{1, -1\}$. It follows from the implementation of $\sigma(t)$, $\phi(t)$ and $s(t)$ that the last two signals depend on $(x(t), y(t), \sigma(t))$, and are not included in the final variables of atan3, which will be presented in the next paragraph.

Now, to explore the calculation of atan3 in computers, which is equal to finding the discrete expressions of $\sigma(t)$, $\phi(t)$, and $s(t)$. Taking the sampling interval δ and letting $t_k = k\delta$ $(k = 1, 2, \ldots)$, then the implementation of $\sigma(t)$ is

$$\sigma(t_{k+1}) = \sigma(t_k)\mathrm{sign}\left(\frac{2\pi}{3} - |\phi(t_k)|\right),$$
$$\phi(t_k) = \mathrm{atan2}(\sigma(t_k)y(t_k), \sigma(t_k)x(t_k))$$

with $\sigma(0) = \mathrm{sign}(2\pi/3 - |\mathrm{atan2}(y_0, x_0)|)$, and the implementation of $s(t)$ is

$$s(t_{k+1}) = s(t_k) + \frac{1}{2}\left(1 - \mathrm{sign}\left(\frac{2\pi}{3} - |\phi(t_k)|\right)\right)$$

with $s(0) = 0$, which leads to the main body of the program. From the implementation of the signals, it can be understood that atan3 depends on (x, y, σ) finally.

Smooth function $\mathrm{atan3}(x(t), y(t), \sigma(t))$ is obtained via cutting and reconnecting $\mathrm{atan2}(y(t), x(t))$ to eliminate its discontinuities, which can be clarified by the following example. In Figure 3, a point moving along an ellipse is expressed as $(x(t), y(t)) = (2\cos t, \sin t)$. Functions $\phi_+(t) = \mathrm{atan2}(y(t), x(t))$ and $\phi_-(t) = \mathrm{atan2}(-y(t), -x(t))$ with step 2π at discontinuities. Function $s(t)\pi$ is piecewise constant with steps π. Argument function $\psi(t)$ is smooth because the steps in $\phi(t)$ are eliminated accurately by steps in $s(t)\pi$. To learn the efficiency of atan3 when the input with uncertainty, let us further consider the situation that $A(t)$ is disturbed by noise $w(t)$. Taking $w(t) = (0.01w_1, 0.005w_2)$ with w_1 and w_2 being independent standard white noises, the results are presented in Figure 4, from which it can be seen that function atan3 is not sensitive to disturbances. Undesirable behavior of atan2 function was pointed out in [33, (181)], and it is modified to $\mathrm{atan2}(y, x) + 2m\pi$ with an integer m, while the second result in Figure 4 indicates the non-feasibility of this direct compensation.

Consider the analytical properties of $\psi(t)$ in t. Since $\mathrm{atan3}(x(t), y(t), \sigma(t))$, $\mathrm{atan2}(y(t), x(t))$, and $\mathrm{atan}(y(t)/x(t))$ differ with only constants at discontinuous points in time of the last two functions, we have

$$\begin{aligned}\dot{\psi}(t) &= \frac{1}{x^2(t) + y^2(t)}\left(-y(t)\dot{x}(t) + x(t)\dot{y}(t)\right), \\ t &\in \{s \geqslant 0 : (x(s), y(s)) \in \mathbb{R}^2/(0,0)^\top\},\end{aligned} \tag{9}$$

which is perfectly consistent with the physical character of the smooth movement.

Remark 2. It can be seen from (9) that when a point tends to the origin, the derivative of atan3 will change dramatically unless its speed converges to zero faster. The origin is often the equilibrium point of the closed-loop system, which brings forth many challenges in controller design.

3 Hierarchical controller design

The hierarchical controller to be designed for a nonholonomic mobile robot is composed of a planner, a position module (innerloop), and an attitude module (outerloop).

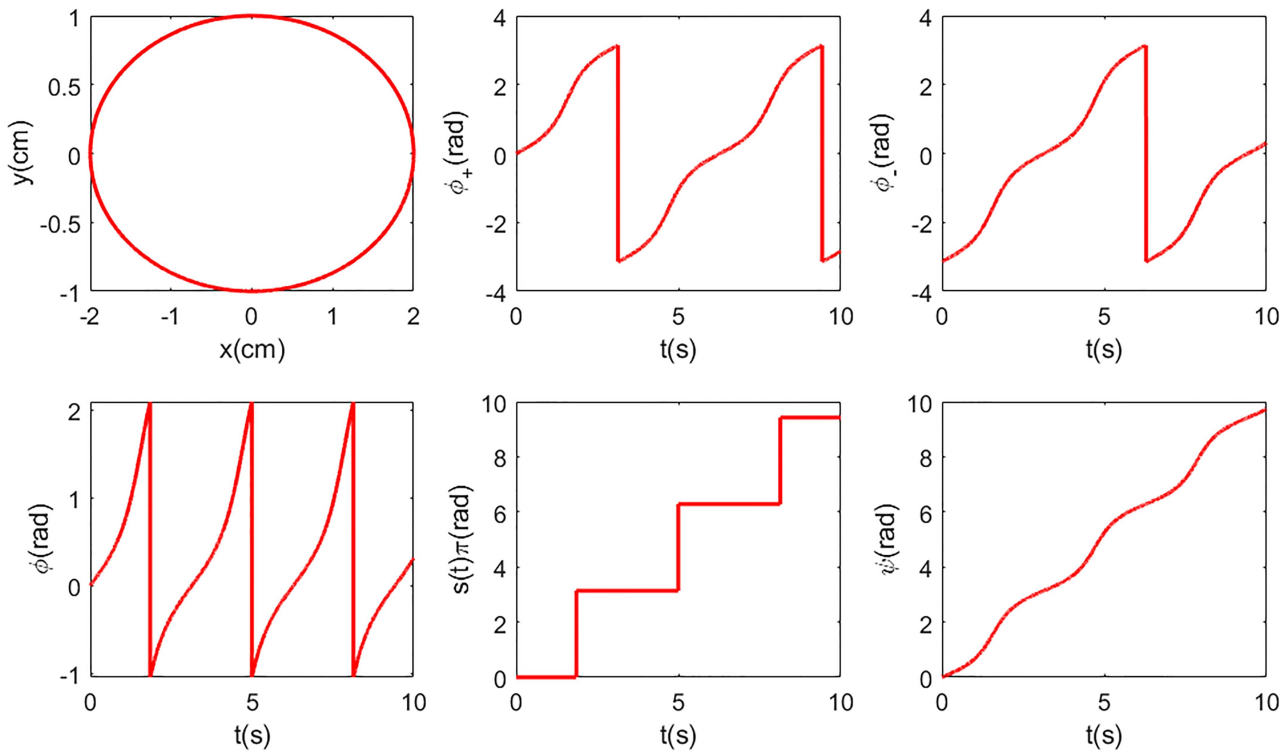

Figure 3 (Color online) Example of two discontinuous functions being switched to a smooth one.

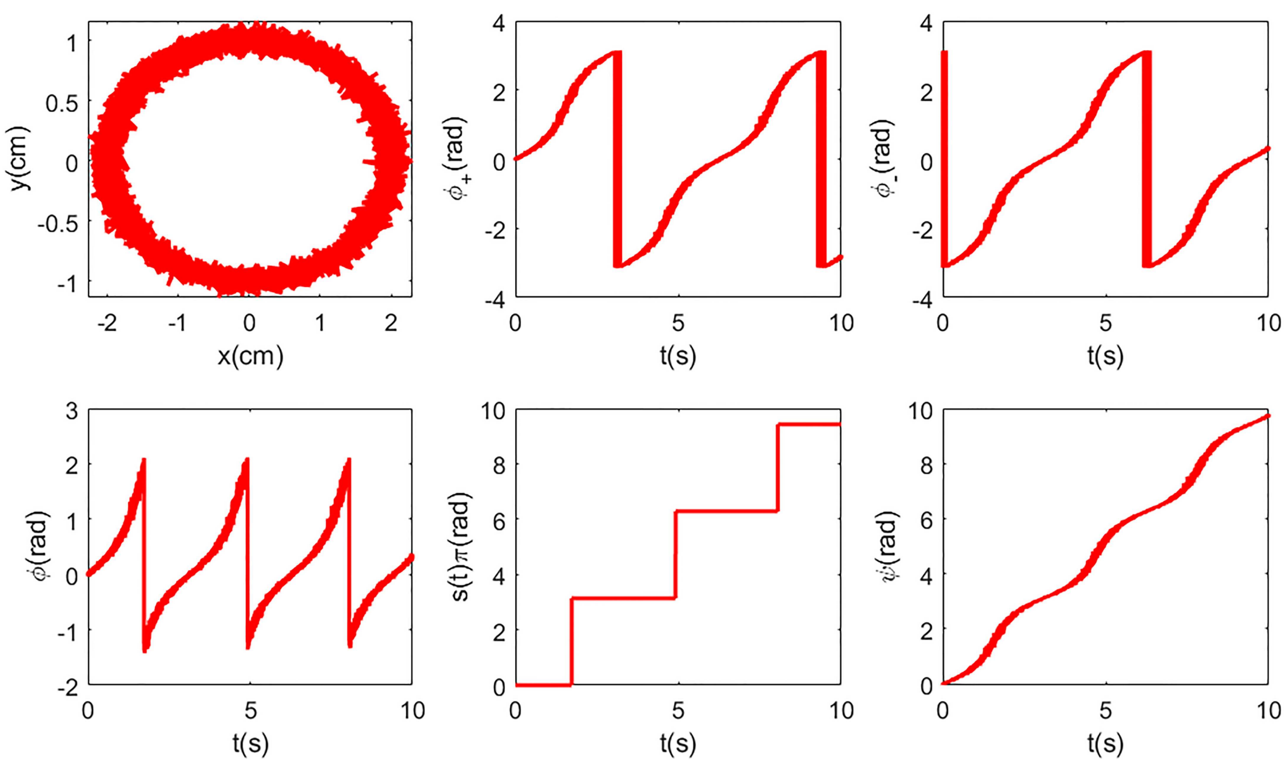

Figure 4 (Color online) The example in Figure 3 is disturbed by noise.

3.1 Planner design

Planners of yaw angle and the translational velocity are designed by introducing a transform of the translational subsystem from under-actuated to full-actuated.

Kinematics equation of (2a) is rewritten in the form of full-actuated

$$\dot{r} = \mu \tag{10}$$

with

$$\mu = v\Lambda(\psi). \tag{11}$$

Here μ is regarded as a virtual control for (10), and is to be designed later as μ_d (see (23)), which can be rewritten as

$$\mu_d = v_d \Lambda\left(\psi_d\right), \tag{12}$$

where ψ_d is the desired yaw angle, and v_d is the desired translational velocity, or expressed as

$$\begin{aligned} \mu_{dx} &= v_d \cos\psi_d, \\ \mu_{dy} &= v_d \sin\psi_d. \end{aligned} \tag{13}$$

In fact, according to (13), for a given μ_d, we can define the desired attitude

$$\psi_d = \text{atan3}\left(\mu_{dx}, \mu_{dy}, \sigma\right), \tag{14}$$

which is called as attitude planner and the desired speed

$$v_d = \sqrt{\mu_{dx}^2 + \mu_{dy}^2}, \tag{15}$$

for all $t \in \{s \geqslant 0 : (x(s), y(s)) \in \mathbb{R}^2/(0,0)\}$.

3.2 Position module design

For the given reference signal r_* and the desired velocity v_d, translational error variables are introduced as

$$\begin{aligned} \tilde{r} &= r - r_*, \\ \tilde{v} &= v - v_d. \end{aligned} \tag{16}$$

From (10) and (2a), the derivative of (16) is derived as

$$\begin{aligned} \dot{\tilde{r}} &= \mu_d - \dot{r}_* + \tilde{\mu} + \Delta, \\ \dot{\tilde{v}} &= p_1 F - \frac{k_0}{m_1}\omega^2 - k_1 v - \dot{v}_d, \end{aligned} \tag{17}$$

where $\Delta = \bar{\mu}_d - \mu_d, \tilde{\mu} = \mu - \bar{\mu}_d$, and $\bar{\mu}_d = v_d \Lambda\left(\psi\right)$. It can be verified that

$$\Delta = 2v_d \begin{bmatrix} -\sin\left(\frac{\psi+\psi_d}{2}\right) \\ \cos\left(\frac{\psi+\psi_d}{2}\right) \end{bmatrix} \sin\left(\frac{\tilde{\psi}}{2}\right) \tag{18}$$

and

$$\tilde{r}^\top \Delta \leqslant \frac{1}{4d_1}|\tilde{r}|^2 + d_1 (v_d)^2 \tilde{\psi}^2, \tag{19}$$

where $\tilde{\psi} = \psi - \psi_d$, $d_1 > 0$ is a design parameter, and that

$$\tilde{\mu} = (v - v_d)\Lambda\left(\psi\right) = \tilde{v}\Lambda\left(\psi\right). \tag{20}$$

Define Lyapunov function for the translational subsystem as

$$V_1 = \frac{1}{2}\tilde{r}^\top \tilde{r} + \frac{1}{2p_1}\tilde{v}^2, \tag{21}$$

whose derivative along (17) with respect to time satisfies

$$\begin{aligned}\dot{V}_1 =& \tilde{r}^\top(\mu_d - \dot{r}_* + \tilde{\mu} + \Delta) \\ &+ \tilde{v}\frac{1}{p_1}\left(p_1 F - \frac{k_0}{m_1}\omega^2 - k_1 v - \dot{v}_d\right) \\ \leqslant& \ \tilde{r}^\top\left(\mu_d - \dot{r}_* + \frac{1}{4d_1}\tilde{r}\right) + d_1(v_d)^2\tilde{\psi}^2 \\ &+ \tilde{v}\left(F + \tilde{r}^\top\Lambda(\psi) - \frac{1}{p_1}\dot{v}_d - \frac{k_0}{m_1 p_1}\omega^2 - \frac{k_1}{p_1}v\right),\end{aligned} \tag{22}$$

where Eqs. (19) and (20) are used. By selecting translational control

$$\begin{aligned}\mu_d =& -\left(c_r + \frac{1}{4d_1}\right)\tilde{r} + \dot{r}_*, \\ F =& -c_v\tilde{v} - \tilde{r}^\top\Lambda(\psi) + \frac{1}{p_1}\dot{v}_d + \frac{k_0}{m_1 p_1}\omega^2 + \frac{k_1}{p_1}v,\end{aligned} \tag{23}$$

where $c_r > 0$ and $c_v > 0$ are design parameters such that (22) becomes

$$\dot{V}_1 \leqslant -c_r|\tilde{r}|^2 - c_v\tilde{v}^2 + d_1(v_d)^2\tilde{\psi}^2. \tag{24}$$

Remark 3. By introducing μ_d, position control is transformed into a form of full-actuated control with Δ regarded as a disturbance that is separated into two terms $|\tilde{r}|^2/4d_1$ and $d_1(v_d)^2\tilde{\psi}^2$. The first term leads to linear damping $(-\tilde{r}/4d_1)$ in (23), and the second term will be dealt with by introducing damping in the attitude controller in the next subsection.

3.3 Attitude module design

Regarding the output ψ_d of the attitude planner as a reference signal, the error variables are introduced as follows:

$$\begin{aligned}\tilde{\psi} &= \psi - \psi_d, \\ \tilde{\omega} &= \omega - \omega_d,\end{aligned} \tag{25}$$

where ω_d is the desired angular velocity to be designed. Taking the derivative of (25) along with (2) yields

$$\begin{aligned}\dot{\tilde{\psi}} &= \omega_d - \dot{\psi}_d + \tilde{\omega}, \\ \dot{\tilde{\omega}} &= p_2\Gamma + \frac{k_0}{m_2}v\omega - k_2\omega - \dot{\omega}_d.\end{aligned} \tag{26}$$

Select Lyapunov function for subsystem (25) as

$$V_2 = \frac{1}{2}\tilde{\psi}^2 + \frac{1}{2p_2}\tilde{\omega}^2 \tag{27}$$

whose derivative along (26) satisfies

$$\dot{V}_2 = \tilde{\psi}(\omega_d - \dot{\psi}_d + \tilde{\omega}) + \tilde{\omega}\left(\Gamma - \frac{1}{p_2}\dot{\omega}_d + \frac{k_0}{m_2 p_2}v\omega - \frac{k_2}{p_2}\omega\right). \tag{28}$$

By designing controller

$$\begin{aligned}\omega_d &= -c_\psi\tilde{\psi} + \dot{\psi}_d - d_1(v_d)^2\tilde{\psi}, \\ \Gamma &= -c_\omega\tilde{\omega} - \tilde{\psi} + \frac{1}{p_2}\dot{\omega}_d - \frac{k_0}{m_2 p_2}v\omega + \frac{k_2}{p_2}\omega,\end{aligned} \tag{29}$$

where $c_\psi > 0$ and $c_\omega > 0$ are the design parameters, Eq. (28) becomes

$$\dot{V}_2 = -c_\psi\tilde{\psi}^2 - c_\omega\tilde{\omega}^2 - d_1(v_d)^2\tilde{\psi}^2. \tag{30}$$

Remark 4. The reference position $r_* \in \mathbb{R}^2$ in (16) can be specified by the customer, but the desired attitude $\psi_d \in \mathbb{R}$ is generated by the controller itself using (14). This means that the proposed scheme has maneuvering ability on attitude, and the under-actuated robot is controlled in a manner of a full-actuated form.

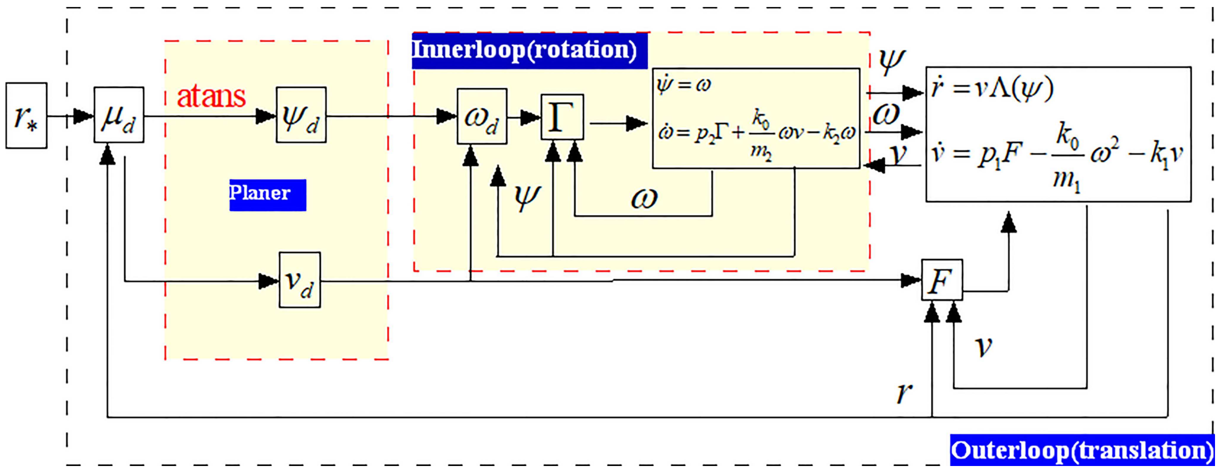

Figure 5 (Color online) Framework of the hierarchical control for WMRs.

3.4 The synthesis of torques

Summarizing planners (14) and (15), translational module (23) and rotational module (29) give the framework of hierarchical control for WMRs, as shown in Figure 5, and then torques as the true controls are synthesized as

$$\tau_1 = F + \Gamma, \quad \tau_2 = F - \Gamma. \tag{31}$$

A closed-loop error system for stability analysis can be obtained by summarizing (2), (23), (26), and (29) as follows:

$$\begin{cases} \dot{\tilde{r}} = -\left(c_r + \dfrac{1}{4d_1}\right)\tilde{r} + \tilde{\mu} + \Delta, \\ \dot{\tilde{v}} = -p_1(c_v\tilde{v} + \tilde{r}^\top\Lambda(\psi)), \\ \dot{\tilde{\psi}} = -c_\psi\tilde{\psi} - d_1(v_d)^2\tilde{\psi} + \tilde{\omega}, \\ \dot{\tilde{\omega}} = -p_2(c_\omega\tilde{\omega} + \tilde{\psi}) \end{cases} \tag{32}$$

whose state is lumped together as $\chi = [\tilde{r}^\top, \tilde{v}^\top, \tilde{\psi}, \tilde{\omega}]^\top$.

4 Performance analysis

By the aid of hierarchical design, we obtain the closed-loop error system whose stability and robustness are to be analyzed based on Lyapunov function in the case of trajectory tracking and stabilization, respectively.

4.1 Stability analysis of trajectory tracking

According to (9) and (14), the analytical properties of v_d are uncertain at the origin, which motivates the following assumption on the trajectory reference signal.

Assumption 1. There exists a positive number ν such that $|\dot{r}_*| \geqslant \nu$ for all $t \in [0, \infty)$.

Theorem 1. For system (2) and r satisfying Assumption 1, smooth control (31) with appropriate design parameters is selected such that the closed-loop system (32) is exponentially stable, and all signals are bounded, with the exception of the angle signals ψ_d and ψ being finite in $[t_0, \infty)$.

Proof. The proof is presented in 4 steps.

(i) Stability of the error system. Lyapunov function of the closed-loop error system (32) is

$$V = V_1 + V_2, \tag{33}$$

whose derivative satisfies

$$\dot{V} \leqslant -c_r|\tilde{r}|^2 - c_v\tilde{v}^2 - c_\psi\tilde{\psi}^2 - c_\omega\tilde{\omega}^2 \leqslant -cV \tag{34}$$

by combining (24) and (30), where $c = 2\min\{c_r, p_1c_v, c_\psi, p_2c_\omega\}$. From (33) and (34), it is easy to obtain that the closed-loop system is exponentially stable, and $\tilde{r}, \tilde{v}, \tilde{\psi}$ and $\tilde{\omega}$ exponentially converge to zero.

(ii) Boundedness of F. The boundedness of r, v_d, and μ_d follows from the definitions themselves and the boundedness of r^* and $\tilde{r}$. It can be concluded from (32) and (31) that $\dot{\tilde{r}}$ and $\dot{\mu}_d$ are bounded, respectively. It comes from the definition of v_d that

$$\dot{v}_d = \frac{1}{\sqrt{\mu_{dx}^2 + \mu_{dy}^2}} [\mu_{dx},\ \mu_{dy}] \dot{\mu}_d. \tag{35}$$

Then we have

$$|\dot{v}_d| \leqslant |\dot{\mu}_d|, \tag{36}$$

which together with the boundedness of $\tilde{v}$ leads to the same property of v. Finally, from the boundedness of ω to be proved in (iii), we can verify that F is bounded by its definition.

(iii) Boundedness of Γ. First, we show v_d is lower bounded by a positive number. Since $|\tilde{r}|$ exponentially converges to zero, there exist constants $\varrho_1 > 0$ and $\varrho_2 > 0$ such that $|\tilde{r}| \leqslant \varrho_1 \mathrm{e}^{-\varrho_2 t}$, and then

$$v_d = |\mu_d| = |-\left(c_r + \frac{1}{4d_1}\right)\tilde{r} + \dot{r}_*| \geqslant |\dot{r}_*| - \left(c_r + \frac{1}{4d_1}\right)\varrho_1 \mathrm{e}^{-\varrho_2 t}.$$

According to the assumption $|\dot{r}_*| \geqslant \nu > 0$, small enough c_r and large enough d_1 can be selected such that

$$v_d \geqslant \nu - \left(c_r + \frac{1}{4d_1}\right)\varrho_1 > 0; \tag{37}$$

i.e., the positive lower boundedness of v_d can be guaranteed.

It is deduced from the derivative of (13) that

$$\begin{aligned} \dot{\mu}_{dx} &= \dot{v}_d \cos\psi_d - v_d \dot{\psi}_d \sin\psi_d, \\ \dot{\mu}_{dy} &= \dot{v}_d \sin\psi_d + v_d \dot{\psi}_d \cos\psi_d, \end{aligned}$$

which gives

$$\dot{\psi}_d = \frac{1}{v_d} \bar{\Lambda}^\top(\psi_d)\dot{\mu}_d, \tag{38}$$

where $\bar{\Lambda}(\psi_d) = [-\sin\psi_d, \cos\psi_d]^\top$. The lower boundedness of v_d and the boundedness of $\dot{\mu}_d$ can guarantee the boundedness of $\dot{\psi}_d$ and $\ddot{\psi}_d$, from which it can be seen that ω_d, ω and $\dot{\omega}_d$ are all bounded. Finally, the boundedness of Γ can be verified by its definition; therefore, τ_1 and τ_2 are bounded.

(iv) Finiteness of angle signals. For any finite-time T, ψ_d is bounded in $[t_0, T]$, then from the boundedness of $\tilde{\psi}$ it is obtained that ψ is bounded on $[t_0, T]$.

Remark 5. The finiteness of angle signals in Theorem 1 can be understood by a simple case. When system (2) rotates around the origin with a constant angular velocity ρ on a circle, argument angle $\psi = \rho(t - t_0)$ is finite rather than bounded while $r = (x, y)^\top$ is bounded on $[t_0, \infty)$.

4.2 Stability analysis of position stabilization

Position stabilization (or the slight general case of set-point regulation) is discussed. It should be pointed out that position stabilization is not performed on the overall system since the desired angle is the output of the planner. Although the stabilization problem naturally does not satisfy the requirements of Assumption 1, it does not mean that the controller designed for the trajectory cannot be used for stabilization problems.

Theorem 2. For system (2), in the case of $\dot{r}_* \equiv 0$, smooth control (31) with appropriate parameters is chosen such that closed-loop error system (32) is exponentially stable, and all signals are bounded, with the exception of the angle signals ψ_d, $\tilde{\psi}$, and ψ being finite in $[t_0, \infty)$.

Proof. The general idea is similar to the proof of the Theorem 1 with the difference in how to prove the boundedness of $\dot{\psi}_d$ by (38) without lower boundedness of v_d. Without loss of generality, $\tilde{\chi}(t_0) \neq 0$ is assumed, then the measure of $\{\tilde{r} : \tilde{r} = 0\}$ equals zero in $\mathbb{R}^2$, so it is possible to assume that $\tilde{r} \neq 0$ during the stabilization process. In fact, from the local Lipschitz condition and the exponential stability of the error closed loop system, the set $S = \{\tilde{\chi} : \tilde{\chi} = 0\}$ cannot be reached in finite time, according to the existence and uniqueness of the solution. The set $S_r = \{\tilde{r} : \tilde{r} = 0\}$ is the equilibrium of $\tilde{r}$-subsystem without input, then $\tilde{r}$ cannot remain in S_r in any finite interval of time, since its inputs (other states of $\tilde{\chi}$-system) are not zero.

According to the proof of Theorem 1, the closed-loop system is exponentially stability and $\tilde{r}, \tilde{v}, \tilde{\psi}$, and $\tilde{\omega}$ exponentially converge to zero. To get the conclusion of Theorem 2, we only need to focus on the situation near the equilibrium point, i.e., the limit case. Letting the right-hand side of (32) ($\dot{r}_* \equiv 0$) equal zero, the convergence rate towards equilibrium of the related variables can be verified. In particular, we have

$$\lim_{t\to\infty} \frac{|\tilde{v}|}{|\tilde{r}|} \leqslant \frac{1}{c_v}, \tag{39}$$

which, together with

$$v_d = |\mu_d| = \left(c_r + \frac{1}{4d_1}\right)|\tilde{r}|, \tag{40}$$

and the definition of $\tilde{\mu}$, implies

$$\lim_{t\to\infty} \frac{|\tilde{\mu}|}{v_d} \leqslant \frac{4d_1}{4d_1c_r+1} \lim_{t\to\infty} \frac{|\tilde{v}|}{|\tilde{r}|} \leqslant \frac{4d_1}{c_v(4d_1c_r+1)}. \tag{41}$$

From the definition of Δ and $\tilde{\psi}$ tending to zero, we have

$$\lim_{t\to\infty} \frac{|\Delta|}{v_d} = 0. \tag{42}$$

Reviewing (38), (23) and (32), one can get

$$\begin{aligned} \dot{\psi}_d &= \frac{1}{v_d}\bar{\Lambda}^\top \dot{\mu}_d = -\left(c_r + \frac{1}{4d_1}\right)\frac{1}{v_d}\bar{\Lambda}^\top \dot{\tilde{r}} \\ &= \left(c_r + \frac{1}{4d_1}\right)\bar{\Lambda}^\top \left(\left(c_r + \frac{1}{4d_1}\right)\frac{\tilde{r}}{v_d} - \frac{\Delta}{v_d} - \frac{\tilde{\mu}}{v_d}\right). \end{aligned} \tag{43}$$

Substituting (40)–(42) into (43) yields

$$\lim\nolimits_{t\to\infty} |\dot{\psi}_d| \leqslant c_r + \frac{1}{4d_1} + \frac{1}{c_v}. \tag{44}$$

The rest is the same as Theorem 1.

4.3 Robust against disturbances

The robustness analysis is also performed in two cases: trajectory tracking and stabilization.

When system (1) is disturbed by noise, the dynamic equation (2) is turned to

$$\begin{aligned} &\dot{r} = v\Lambda(\psi), \\ &\dot{\psi} = \omega, \\ &\dot{v} = p_1F - \frac{k_0}{m_1}\omega^2 - k_1v + d_v, \\ &\dot{\omega} = p_2\Gamma + \frac{k_0}{m_2}v\omega - k_2\omega + d_\omega, \end{aligned} \tag{45}$$

where unknown functions d_v and d_ω are bounded; i.e., there exist constants $\bar{d}_v$ and $\bar{d}_\omega$ such that

$$|d_v| \leqslant \bar{d}_v, \quad |d_\omega| \leqslant \bar{d}_\omega.$$

Adding nonlinear damping terms to (31) results in a robust controller

$$\begin{aligned} &\tau_1 = F + \Gamma, \quad \tau_2 = F - \Gamma, \\ &F = -(c_v + d_2)\tilde{v} - \tilde{r}^\top\Lambda(\psi) + \frac{1}{p_1}\dot{v}_d + \frac{k_0}{m_1p_1}\omega^2 + \frac{k_1}{p_1}v, \\ &\Gamma = -(c_\omega + d_3)\tilde{\omega} - \tilde{\psi} + \frac{1}{p_2}\dot{\omega}_d - \frac{k_0}{m_2p_2}v\omega + \frac{k_2}{p_2}\omega, \end{aligned} \tag{46}$$

where $d_2, d_3 \geqslant 0$ are design parameters.

With respect to the trajectory tracking, the robust adaptive controller possesses the following properties.

Theorem 3. For system (45) and r_* satisfying Assumption 1, a smooth control (46) with appropriate design parameters is selected such that all signals are bounded except that the angle signals ψ_d and ψ are finite in $[t_0, \infty)$. The tracking error can be made arbitrarily small by tuning design parameters.

Proof. The derivative of (33) satisfies

$$\dot{V} \leqslant -cV + d, \tag{47}$$

where $d = \bar{d}_v^2/4d_2 + \bar{d}_\omega^2/4d_3$. According to the assumption $|\dot{r}_*| \geqslant \nu > 0$, as in (37), a small enough c_r and a large enough d_i $(i = 1, 2, 3)$ can be chosen such that

$$v_d \geqslant \nu - \left(c_r + \frac{1}{4d_1}\right)\varrho_1 - \bar{d} > 0, \tag{48}$$

where $\bar{d}$ depends on d/c; i.e., the positive lower boundedness of v_d can be guaranteed by selecting controller parameters.

With respect to the set-point regulation/stabilization, the robust adaptive controller has the following properties.

Theorem 4. For system (2), in the case of $\dot{r}_* \equiv 0$, a smooth control (46) with appropriately designed parameters is selected such that in the closed-loop system,

(1) signals r, v_d, v, and F are bounded,

(2) the tracking error can be made arbitrarily small by tuning design parameters, and

(3) the angle signals ψ_d, ψ, ω_d, and Γ are finite.

Proof. Proof of (1) and (2) is similar to the tracking case and is omitted, and only outline (3) is presented. Without loss of generality, it can be assumed that the existence of disturbance will avoid the state staying at the origin for a finite interval; i.e., the measure of $v_d = 0$ equals zero. Therefore, in any finite interval, the existence of ψ_d can be guaranteed, then ψ is finite, which means the variables in Γ are finite, then Γ is finite.

Remark 6. Compared with Theorem 3, no lower boundedness of v_d can be obtained in Theorem 4, then only finiteness of Γ is proved in the case of stabilization and regulation. In practice, for a short interval $[t_0, t_0 + T]$, the finiteness can be seen as the boundedness.

Remark 7. By replacing the discontinuous function atan2 with the smooth function atan3, the under-actuated problem can be changed into the full-actuated problem, and a smooth and time-invariant controller is designed. Brockett's condition in [34] shows that nonholonomic systems cannot be stabilized by continuous time-invariant state feedback. The topological obstacles given by [35] indicate that a mechanical system with rotational degrees of freedom does not have a globally asymptotically stable equilibrium point. This result does not contradict with these two references because only position $r = (x, y)$ of configuration $(x, y, \psi)^\top$ is regulated to r_*, and attitude ψ is required to follow the output of the planner.

Consider the realization of some derivative signals in the controller: $\dot{\psi}_d$, $\dot{v}_d$ and $\dot{\omega}_d$. Although the analytic expressions of these signals can be presented by using partial differential operators, such expressions have a complicated structure. This prompts us to introduce filters to obtain satisfactory approximate results. As in [36, 37], three commanding filters are presented as follows:

$$\begin{aligned} \dot{\psi}_d^c &= \kappa_1(-\psi_d^c + \psi_d), \\ \dot{v}_d^c &= \kappa_2(-v_d^c + v_d), \\ \dot{\omega}_d^c &= \kappa_3(-\omega_d^c + \omega_d), \end{aligned} \tag{49}$$

where sufficiently large κ_i $(i = 1, 2, 3)$ is required, then ψ_d, v_d, and ω_d in controller can be replaced respectively by ψ_d^c, v_d^c, and ω_d^c, respectively, therefore results in Theorems 3 and 4 are still valid.

5 Adaptive control

In system (2), parameters p_1, p_2, k_1, and k_2 are determined by the radius and the inertia of the wheel, the mass, the inertia and the width of the vehicle, the resistance coefficient, which often change from the normal values. In an extreme case of all system parameters of WMRs being unknown, an adaptive controller is designed to perform stabilization and trajectory tracking.

Assumption 2. For system (45), p_1, p_2, k_1, and k_2 are all unknown constants.

In (31), the controller $\tau = (\tau_1, \tau_2)^\top$ can be rewritten as

$$\begin{aligned} &\tau_1 = F + \Gamma,\ \ \tau_2 = F - \Gamma, \\ &F = -c_v\tilde{v} - \tilde{r}^\top\Lambda(\psi) + \theta_1^\top\Phi_1, \\ &\Gamma = -c_\omega\tilde{\omega} - \tilde{\psi} + \theta_2^\top\Phi_2, \end{aligned} \tag{50}$$

where $\Phi_1 = [\omega^2, v, \dot{v}_d]^\top$, $\Phi_2 = [-v\omega, \omega, \dot{\omega}_d]^\top$, and the lumping parameters θ_1 and θ_2 are

$$\theta_1 = \left[\frac{k_0}{m_1p_1}, \frac{k_1}{p_1}, \frac{1}{p_1}\right]^\top, \quad \theta_2 = \left[\frac{k_0}{m_2p_2}, \frac{k_2}{p_2}, \frac{1}{p_2}\right]^\top$$

which prompt us to construct adaptive laws for θ_1 and θ_2 when they are unknown.

Lyapunov function can be obtained by adding the adaptive error terms to the original form as

$$V = \frac{1}{2}\tilde{r}^\top\tilde{r} + \frac{1}{2p_1}\tilde{v}^2 + \frac{1}{2}\gamma_1\tilde{\theta}_1^\top\tilde{\theta}_1 + \frac{1}{2}\tilde{\psi}^2 + \frac{1}{2p_2}\tilde{\omega}^2 + \frac{1}{2}\gamma_2\tilde{\theta}_2^\top\tilde{\theta}_2, \tag{51}$$

where $\tilde{\theta}_1 = \hat{\theta}_1 - \theta_1$, $\tilde{\theta}_2 = \hat{\theta}_2 - \theta_2$, $\hat{\theta}_1$ and $\hat{\theta}_2$ are estimates of θ_1 and θ_2, respectively, and $\gamma_1 > 0, \gamma_2 > 0$ are design parameters. The derivative of (51) along with (32) satisfies

$$\begin{aligned} \dot{V} = {}& \tilde{r}^\top(\mu_d - \dot{r}_* + \tilde{\mu} + \Delta) \\ & + \tilde{v}\left(F + \frac{k_0}{m_1p_1}\omega^2 - \frac{k_1}{p_1}v - \frac{1}{p_1}\dot{v}_d\right) \\ & + \gamma_1\tilde{\theta}_1^\top\dot{\hat{\theta}}_1 + \tilde{\psi}(\omega_d - \dot{\psi}_d + \tilde{\omega}) \\ & + \tilde{\omega}\left(\Gamma - \frac{k_0}{p_2}v\omega - \frac{k_2}{m_2p_2}\omega - \frac{1}{p_2}\dot{\omega}_d\right) + \gamma_2\tilde{\theta}_2^\top\dot{\hat{\theta}}_2. \end{aligned} \tag{52}$$

Following a similar line as that in the last section, one can derive

$$\begin{aligned} \dot{V} \leqslant {}& \tilde{r}^\top\left(\mu_d - \dot{r}_* + \frac{1}{4d_1}\tilde{r}\right) \\ & + \tilde{v}(F + \tilde{r}^\top\Lambda(\psi) - \theta_1^\top\Phi_1) \\ & + d_1(v_d)^2\tilde{\psi}^2 + \gamma_1\tilde{\theta}_1^\top\dot{\hat{\theta}}_1 + \tilde{\psi}(\omega_d - \dot{\psi}_d) \\ & + \tilde{\omega}(\Gamma + \tilde{\psi} - \theta_2^\top\Phi_2) + \gamma_2\tilde{\theta}_2^\top\dot{\hat{\theta}}_2. \end{aligned} \tag{53}$$

Select a robust adaptive control as

$$\begin{aligned} &F = -(c_v + d_2)\tilde{v} - \tilde{r}^\top\Lambda(\psi) + \hat{\theta}_1^\top\Phi_1, \\ &\Gamma = -(c_\omega + d_3)\tilde{\omega} - \tilde{\psi} + \hat{\theta}_2^\top\Phi_2, \\ &\dot{\hat{\theta}}_1 = -\sigma_1\hat{\theta}_1 + \tilde{v}\gamma_1^{-1}\Phi_1, \\ &\dot{\hat{\theta}}_2 = -\sigma_2\hat{\theta}_2 + \tilde{\omega}\gamma_2^{-1}\Phi_2, \end{aligned} \tag{54}$$

where $\sigma_1, \sigma_2 \geqslant 0$, $\gamma_1, \gamma_2 > 0$ are design parameters, such that Eq. (53) can be rewritten as

$$\begin{aligned} \dot{V} \leqslant {}& -c_r|\tilde{r}|^2 - c_v\tilde{v}^2 - c_\psi\tilde{\psi}^2 - c_\omega\tilde{\omega}^2 \\ & - \frac{1}{2}\sigma_1\gamma_1|\tilde{\theta}_1|^2 - \frac{1}{2}\sigma_2\gamma_2|\tilde{\theta}_2|^2 + \frac{1}{4d_2}\bar{d}_v^2 \\ & + \frac{1}{4d_3}\bar{d}_\omega^2 + \frac{1}{2}\sigma_1\gamma_1|\theta_1|^2 + \frac{1}{2}\sigma_2\gamma_2|\theta_2|^2 \\ \leqslant {}& -cV + d, \end{aligned} \tag{55}$$

where $c = \min\{2c_r, 2p_1c_v, 2c_\psi, 2p_2c_\omega, \sigma_1, \sigma_2\}$ and $d = \frac{\bar{d}_v^2}{4d_2} + \frac{\bar{d}_\omega^2}{4d_3} + \frac{1}{2}\sigma_1\gamma_1|\theta_2|^2 + \frac{1}{2}\sigma_2\gamma_2|\theta_2|^2$.

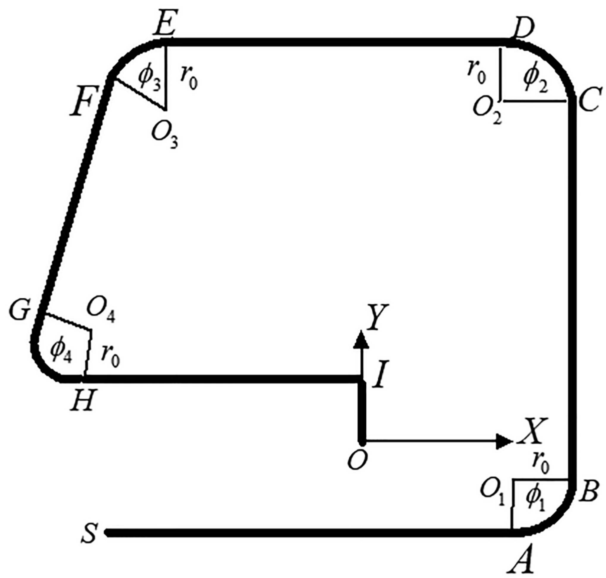

Figure 6 Drive WMRs along a prescribed trajectory.

Closed-loop error system for stability analysis can be summarized as follows:

$$\begin{cases} \dot{\tilde{r}} = -\left(c_r + \dfrac{1}{4d_1}\right)\tilde{r} + \tilde{\mu} + \Delta, \\ \dot{\tilde{v}} = -c_v\tilde{v} + \tilde{r}^\top \Lambda(\psi) + \tilde{\theta}_1^\top \Phi_1, \\ \dot{\tilde{\psi}} = -c_\psi\tilde{\psi} - d_1(v_d)^2\tilde{\psi} + \tilde{\omega}, \\ \dot{\tilde{\omega}} = -c_\omega\tilde{\omega} - \tilde{\psi} + \tilde{\theta}_2^\top \Phi_2, \\ \dot{\tilde{\theta}}_1 = -\sigma_1\hat{\theta}_1 - \tilde{v}\gamma_1^{-1}\Phi_1, \\ \dot{\tilde{\theta}}_2 = -\sigma_2\hat{\theta}_2 - \tilde{\omega}\gamma_2^{-1}\Phi_2. \end{cases} \tag{56}$$

The following theorem shows that controller (54) satisfies the certain equivalence principle.

Theorem 5. For system (45) under Assumption 1 (or $\dot{r}_* \equiv 0$) and Assumption 2, a smooth control (54) with appropriate design parameters is selected such that all signals of the closed-loop system (56) are bounded except for the angle signals ψ_d and ψ are finite in $[t_0, \infty)$. The tracking error can be made arbitrarily small by tuning design parameters.

Proof. From (51) and (55), the results can be proved by following the same steps as Theorems 1–4.

6 Simulation

In order to demonstrate that the efficiency of the controller proposed, 3 simulations are presented for the same WMRs. The system parameters of system (1) are $l_b = 0.4$, $l_d = 0.1$, $l_w = 0.1$, $m_c = 4$, $m_w = 0.5$, $I_c = 1$, $I_w = 0.001$, $I_m = 0.001$ and damping coefficient $d_p = 0.1$, which mean that $k_0 = 0.005$, $k_1 = 3.937$, $k_2 = 2.2222$, $p_1 = 3.937$, $p_2 = 5.5556$, $\theta_1 = [0.02, 1, 0.254]^\top$, and $\theta_2 = [0.05, 0.4, 0.18]^\top$.

To verify the effectiveness of the adaptive tracking control, we conduct the first simulation.

Simulation 1. As shown in Figure 6, the coordinate system is established as XOY, and the WMR is driven along a prescribed trajectory. Control tasks: The vehicle starts from S to A parallel to the X-axis, then turns to B, through C, D, E, F, G, H in turn, and reaches I. Every turning radius is r_0, the angles of the four corners are ϕ_1 to ϕ_4, and the linear velocity in any stage equals v_s. The travel times in $\overrightarrow{SA}$, $\overrightarrow{AB}$, $\overrightarrow{BC}$, $\overrightarrow{CD}$, $\overrightarrow{DE}$, $\overrightarrow{EF}$, $\overrightarrow{FG}$, $\overrightarrow{GH}$, $\overrightarrow{HI}$ are T_1 to T_9, respectively. All parameters of the system are unknown for the designer of the controller. Controller (54) as well as commanding filters in (49) are chosen to achieve the task. During simulation, we take the parameters of trajectory $v_s = 5$, $r_0 = 5.2$, $\phi_1 = \phi_2 = \frac{\pi}{2}$, $\phi_3 = \frac{5\pi}{12}$, $\phi_4 = \frac{7\pi}{12}$, $T_1 = T_3 = T_5 = 10$, $T_7 = 6.3$, $T_9 = 7.3$, and figure out the time of the turn $T_2 = T_4 = \frac{\pi}{10}$, $T_6 = \frac{\pi}{12}, T_8 = \frac{7\pi}{60}$. Controller parameters: $c_r = 0.01$, $c_v = 10$,

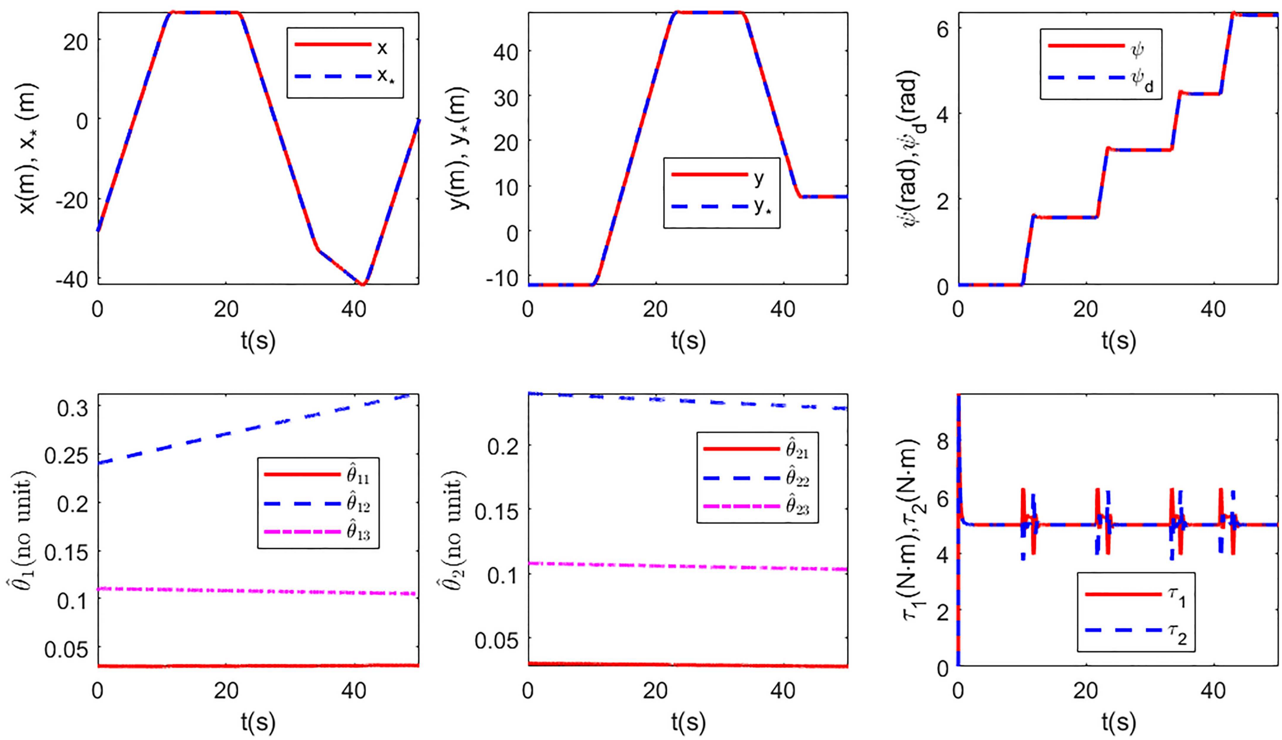

Figure 7 (Color online) Results of Simulation 1: adaptive trajectory tracking control.

$c_\psi = 0.01$, $c_\omega = 10$, $\kappa_1 = \kappa_2 = \kappa_3 = 10$, $d_1 = 0.5$, $d_2 = d_3 = \sigma_1 = \sigma_2 = 0$, $\gamma_1 = \gamma_2 = 10^3$. Initial values: $x_0 = -28.4$, $y_0 = -12$, $v_{x0} = 0$, $v_{y0} = 0$, $\psi_0 = 0$, $\omega_0 = 0$ and take initials $\theta_1(0), \theta_2(0)$ as 60% of the true values.

The simulation results are shown in Figure 7. The torque is larger in the initial stage and at the turning points, which is completely consistent with the experience of human driving.

To verify the necessity of introducing atan3, we present the second simulation.

Simulation 2. In Simulation 1, atan3 in control (54) is replaced with atan2; i.e., let

$$\psi_d = \operatorname{atan2}\left(\mu_{dy}(t), \mu_{dx}(t)\right),$$

the rest remains unchanged, and the simulation results are shown in Figure 8. When ψ first reaches π at about moment 23.5, the robot begins trapping in intense oscillations. This shows the necessity of introducing atan3 to replace the traditional function atan2.

To show the compatibility of the controller on trajectory tracking and stabilization, we perform the third simulation.

Simulation 3. A new task is added to Simulation 1: once the vehicle reaches point I, it is further stabilized at the origin O during the time interval T_{10}. Let $T_{10} = 4$ and set controller parameters to be the same as in Simulation 1. Simulation results are shown in Figure 9, and it can be seen that there are overshoots of torques in the initial stage of the stabilization. This means that we can perform the trajectory tracking and stabilization with the same control.

Other simulations, such as robustness, can be performed and are omitted due to space limitations.

7 Conclusion

In this paper, the unified design of a trajectory tracking and stabilization controller for nonholonomic WMRs based on an attitude planner is studied. To this end, via switching between two discontinuous functions with 180° phase difference, a smooth argument function atan3 with range $(-\infty, \infty)$ is obtained, as the generalization of atan2 with range $(-\pi, \pi)$ and atan with $(-\pi/2, \pi/2)$. The attitude planner is constructed based on atan3, such that the yaw angle becomes a maneuvering variable and under-actuated control turns into a full-actuation form, which results in a hierarchical control, a standard modular design. As one advantage of the modular design, the controller can be retrofitted for WMRs with unknown parameters and disturbances. Wide applications of the mathematical tool

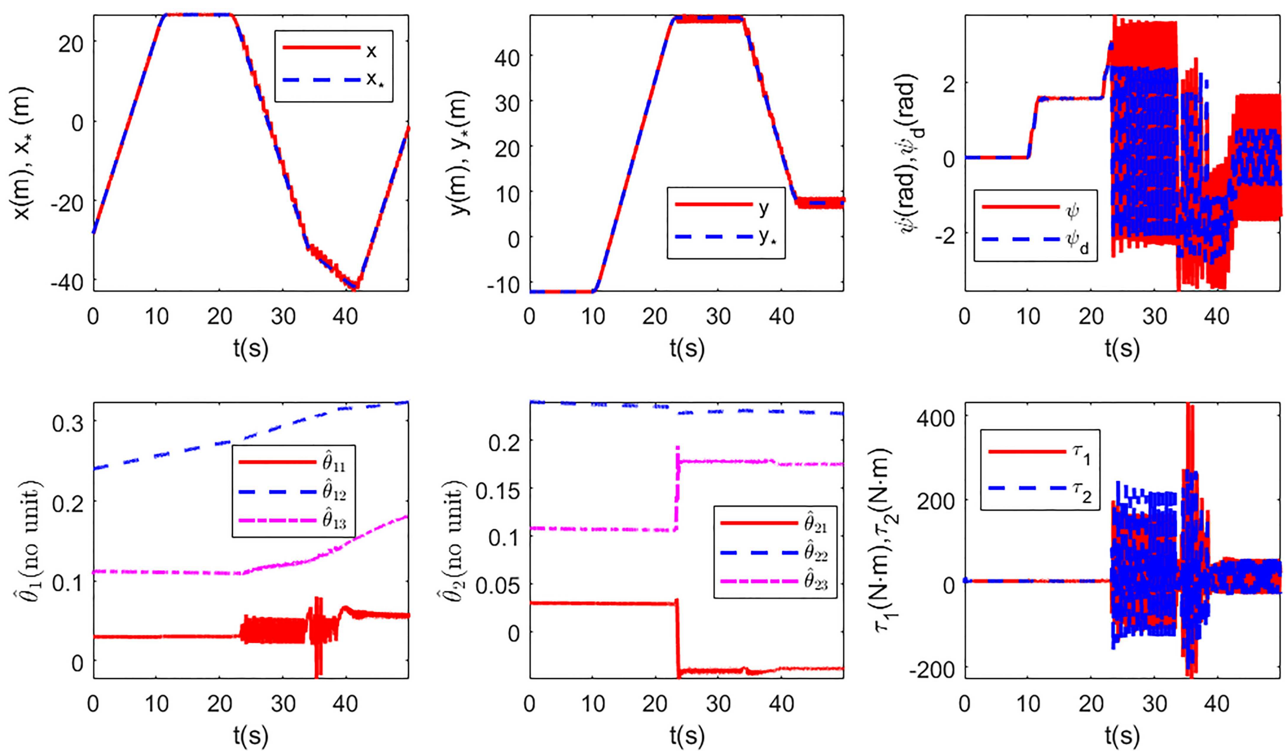

Figure 8 (Color online) Results of Simulation 2: performance degradation due to replacing atan3 with atan2.

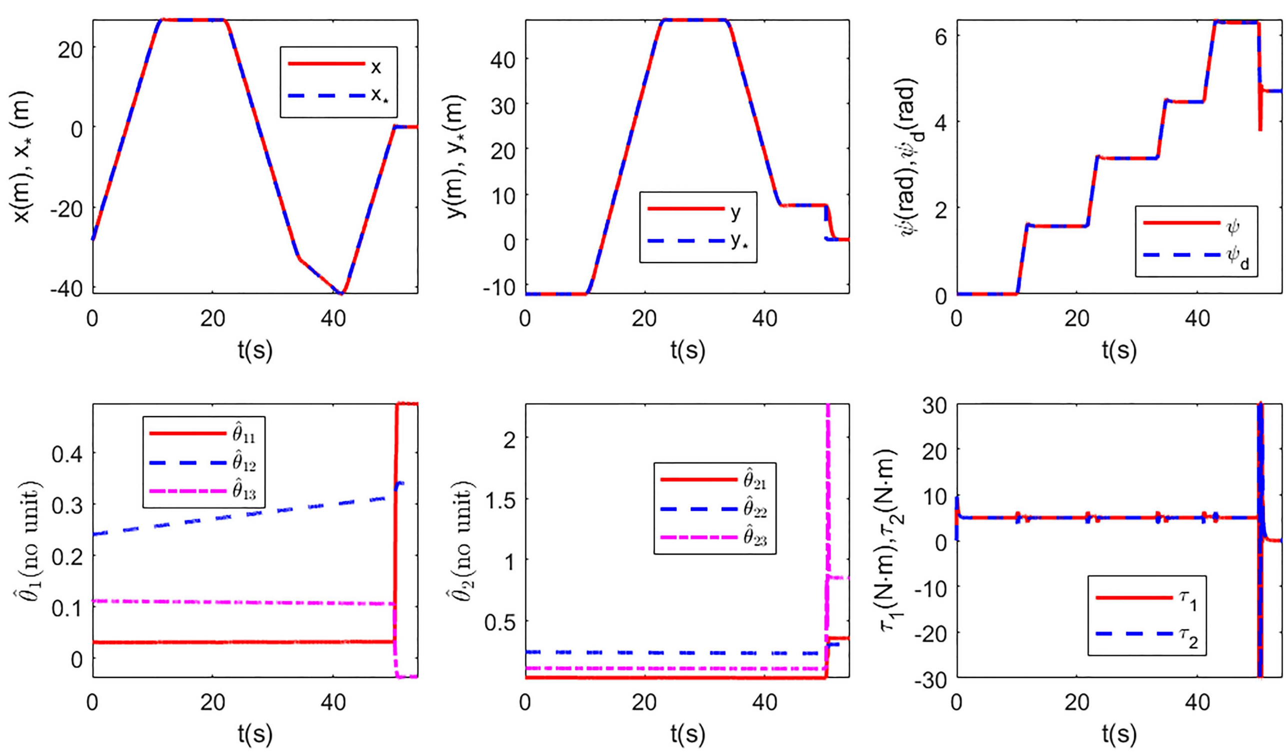

Figure 9 (Color online) Results of Simulation 3: trajectory tracking is augmented by adding a regulating procedure (last for 4 s).

atan3 are to be found in the future, such as exploring to resolve topological obstacle problems, such as the deadlock and the unwind in attitude control researched in [38, 39].

Acknowledgements This work was supported by National Natural Science Foundation of China (Grant No. 62073275).

References

1 Brockett R W. Asymptotic stability and feedback stabilization. Differential Geom Control Theory, 1983, 27: 181–191
2 Murray R M, Sastry S S. Nonholonomic motion planning: steering using sinusoids. IEEE Trans Automat Control, 1993, 38: 700–716
3 Kolmanovsky I, McClamroch N H. Developments in nonholonomic control problems. IEEE Control Syst, 1995, 15: 20–36
4 Bloch A M, Reyhanoglu M, McClamroch N H. Control and stabilization of nonholonomic dynamic systems. IEEE Trans Automat Control, 1992, 37: 1746–1757
5 de Wit C C, Sordalen O J. Exponential stabilization of mobile robots with nonholonomic constraints. IEEE Trans Automat Control, 1992, 37: 1791–1797
6 Walsh G, Tilbury D, Sastry S, et al. Stabilization of trajectories for systems with nonholonomic constraints. IEEE Trans Automat Control, 1994, 39: 216–222
7 Samson C. Control of chained systems application to path following and time-varying point-stabilization of mobile robots. IEEE Trans Automat Control, 1995, 40: 64–77
8 Jiang Z P. Iterative design of time-varying stabilizers for multi-input systems in chained form. Systems Control Lett, 1996, 28: 255–262
9 Godhavn J M, Egeland O. A Lyapunov approach to exponential stabilization of nonholonomic systems in power form. IEEE Trans Automat Control, 1997, 42: 1028–1032
10 M'Closkey R T, Murray R M. Exponential stabilization of driftless nonlinear control systems using homogeneous feedback. IEEE Trans Automat Control, 1997, 42: 614–628
11 Wang C. Semiglobal practical stabilization of nonholonomic wheeled mobile robots with saturated inputs. Automatica, 2008, 44: 816–822
12 Urakubo T. Feedback stabilization of a nonholonomic system with potential fields: application to a two-wheeled mobile robot among obstacles. Nonlinear Dynam, 2015, 81: 1475–1487
13 Corke P. Robotics, Vision and Control: Fundamental Algorithms in MATLAB. Cham: Springer, 2023
14 Duan G R. A FAS approach for stabilization of generalized chained forms: part 1. Discontinuous control laws. Sci China Inf Sci, 2024, 67: 122201
15 Duan G R. A FAS approach for stabilization of generalized chained forms: part 2. Continuous control laws. Sci China Inf Sci, 2024, 67: 132201
16 Jiang Z P, Nijmeijer H. Tracking control of mobile robots: a case study in backstepping. Automatica, 1997, 33: 1393–1399
17 Jiang Z P, Nijmeijer H. A recursive technique for tracking control of nonholonomic systems in chained form. IEEE Trans Automat Control, 1999, 44: 265–279
18 Fukao T, Nakagawa H, Adachi N. Adaptive tracking control of a nonholonomic mobile robot. IEEE Trans Robot Automat, 2000, 16: 609–615
19 Dong W J, Kuhnert K D. Robust adaptive control of nonholonomic mobile robot with parameter and nonparameter uncertainties. IEEE Trans Robot, 2005, 21: 261–266
20 Huang J, Wen C, Wang W, et al. Adaptive output feedback tracking control of a nonholonomic mobile robot. Automatica, 2014, 50: 821–831
21 Yan L, Ma B, Jia Y. Trajectory tracking control of nonholonomic wheeled mobile robots using only measurements for position and velocity. Automatica, 2024, 159: 111374
22 Tayebi A, Rachid A. A unified discontinuous state feedback controller for the path-following and the point-stabilization problems of a unicycle-like mobile robot. In: Proceedings of the 1997 IEEE International Conference on Control Applications, Hartford, 1997. 31–35
23 Dixon W E, Jiang Z P, Dawson D M. Global exponential setpoint control of wheeled mobile robots: a Lyapunov approach. Automatica, 2000, 36: 1741–1746
24 Dixon W E, Dawson D M, Zergeroglu E, et al. Nonlinear Control of Wheeled Mobile Robots. London: Springer, 2001
25 Do K D, Jiang Z P, Pan J. Simultaneous tracking and stabilization of mobile robots: an adaptive approach. IEEE Trans Automat Control, 2004, 49: 1147–1152
26 Li J W. Adaptive tracking and stabilization of nonholonomic mobile robots with input saturation. IEEE Trans Automat Control, 2021, 67: 6173–6179
27 El-Hawwary M I, Maggiore M. Reduction theorems for stability of closed sets with application to backstepping control design. Automatica, 2013, 49: 214–222
28 Roza A, Maggiore M. A class of position controllers for underactuated VTOL vehicles. IEEE Trans Autom Control, 2014, 59: 2580–2585
29 Naldi R, Furci M, Sanfelice R G, et al. Robust global trajectory tracking for underactuated VTOL aerial vehicles using inner-outer loop control paradigms. IEEE Trans Automat Control, 2017, 62: 97–112
30 Invernizzi D, Lovera M, Zaccarian L. Integral ISS-based cascade stabilization for vectored-thrust UAVs. IEEE Control Syst Lett, 2019, 4: 43–48
31 Sarkar N, Xiaoping Yun N, Kumar V. Control of mechanical systems with rolling constraints. Int J Robotics Res, 1994, 13: 55–69
32 Organick E I. A FORTRAN Primer. Addison-Wesley Series in Computer Science and Information Processing. London: Addison Wesley Longman Publishing, 1963
33 Beard R W, McLain T W. Small Unmanned Aircraft: Theory and Practice. Princeton: Princeton University Press, 2012
34 Brockett R W. Asymptotic stability and feedback stabilization. In: Differential Geometric Control Theory. Boston: Birkhauser, 1983, 181–191
35 Bhat S P, Bernstein D S. A topological obstruction to continuous global stabilization of rotational motion and the unwinding phenomenon. Systems Control Lett, 2000, 39: 63–70
36 Farrell J A, Polycarpou M, Sharma M, et al. Command filtered backstepping. IEEE Trans Automat Control, 2009, 54: 1391–1395
37 Dong W J, Farrell J A, Polycarpou M M, et al. Command filtered adaptive backstepping. IEEE Trans Contr Syst Technol, 2012, 20: 566–580
38 Wen J T Y, Kreutz-Delgado K. The attitude control problem. IEEE Trans Automat Control, 1991, 36: 1148–1162
39 Mayhew C G, Sanfelice R G, Teel A R. Quaternion-based hybrid control for robust global attitude tracking. IEEE Trans Automat Control, 2011, 56: 2555–2566